Redox-responsive Bi- and Tri-nuclear Iron/Molybdenum Complexes incorporating the Ferrocenyl Unit as a Redox Spectator†

Mohan M. Bhadbhade,[a] Amitava Das,*[,a] John C. Jeffery,[b] Jon A. McCleverty,*[,b] Jon A. Navas Badiola[b] and Michael D. Ward*[,b]

[a] *Coordination Chemistry Division, Central Salt and Marine Chemicals Research Institute, Bhavnagar-364002, India*

[b] *School of Chemistry, University of Bristol, Cantock's Close, Bristol BS8 1TS, UK*

Seven new ferrocene derivatives L^1–L^7 with pendant arms containing a terminal 4-pyridyl binding site have been prepared and characterized. Six have one pendant arm, whereas the seventh has two pendant arms, one on each cyclopentadienyl ring. Two have been crystallographically characterized: $(C_5H_5)Fe(C_5H_4)CH{=}CH(4\text{-}C_5H_4N)$ (L^1) and $(C_5H_5)Fe(C_5H_4)(4\text{-}C_6H_4)CH{=}CH(4\text{-}C_5H_4N)$ (L^4). In both cases the conjugated side-arm is approximately planar. Attachment of {MoL*(NO)Cl} fragments [L* = tris(3,5-dimethylpyrazolyl)hydroborate] to the vacant pyridyl sites of L^1–L^7 afforded bimetallic complexes which contain electron-donating ferrocenyl groups attached *via* conjugated bridges to electron-deficient {MoL*(NO)Cl} fragments. The new ferrocenes and complexes were thoroughly characterized by electrochemical, UV/VIS and EPR spectroscopic methods, and significant inter-component interactions are evident: co-ordination of the {MoL*(NO)Cl} fragment results in a shift of the ferrocenyl redox potential to more positive potentials by approximately 40 mV per {MoL*(NO)Cl} substituent; the reductions (from 17 to 18 valence electrons) of the {MoL*(NO)Cl} groups are likewise made less negative by the presence of highly conjugated substituents on their pyridyl ligands. The electronic spectra contain transitions from both the ferrocenyl and the {MoL*(NO)Cl} components which are charge transfer in origin and therefore solvatochromic. The EPR spectra of the binuclear complexes containing one {MoL*(NO)Cl} substituent are entirely normal; however the spectrum of $[\{MoL^*(NO)Cl\}_2L^7]$, which contains two paramagnetic {MoL*(NO)Cl} groups attached to the two pendant arms of L^7, shows a weak magnetic exchange interaction between the paramagnetic centres which must be transmitted through the bridging ligand and across the ferrocenyl unit.

Supramolecular systems containing a number of electronically coupled redox-responsive centres are of considerable current interest owing to the rapid growth of material science.[1–3] Metallocenes and in particular ferrocene have been widely used for designing molecular ferromagnets,[4–6] molecular sensors [7–11] and have been used in the development of optoelectronic devices based on the non-linear polarization of molecular materials.[12–18] The intense interest in using ferrocene as a component of molecular sensors may be ascribed to its unique redox behaviour, remarkable stability, and the ease with which the ferrocene unit may be derivatized. In addition, oxidation of a ferrocenyl unit permits electronic tuning of the properties of a secondary, covalently attached metal fragment.[19–25]

In this paper we describe the preparation of a variety of ferrocene derivatives which contain one or two pendant metal-binding pyridyl sites attached to the ferrocenyl core through a conjugated pathway. The complex $[MoL^*(NO)Cl_2]$ [L* = tris(3,5-dimethylpyrazolyl)hydroborate] is known to form adducts with pyridine (py) or substituted pyridines by loss of a substitution-labile chloride; the resulting complexes [MoL*(NO)Cl(py)] have a 17-electron configuration and are redox active, undergoing one-electron oxidation (17e–16e couple) and reduction (17e–18e couple) processes which are chemically reversible on the electrochemical time-scale.[26–28] We have accordingly linked the 17-electron molybdenum fragment {MoL*(NO)Cl} to these new ferrocene derivatives to construct a series of bi- and tri-nuclear complexes. Electrochemical interactions across conjugated bridging ligands in complexes involving this fragment have been shown to be remarkably strong; in a series of binuclear complexes $[\{MoL^*(NO)Cl\}_2(\mu\text{-}L)]$ (L = 4,4'-bipyridine or an 'extended' analogue) the electrochemical interaction between the remote metal centres, as measured by the separation between the two 17e–18e couples, was approximately an order of magnitude stronger than that in the more well known complexes $[\{Ru(NH_3)_5\}_2(\mu\text{-}L)]^{4+}$.[26–28] We report here the synthesis, characterization and physicochemical properties of the new ferrocene derivatives L^1–L^7 and their respective molybdenum complexes $Mo'L^1$–$Mo'L^6$ and Mo'_2L^7 where Mo' denotes the complex fragment {MoL*(NO)Cl} attached to the pendant pyridyl residues of the ligands.

Experimental

Proton NMR spectra were recorded on JEOL 100 or GX270 spectrometers, fast-atom bombardment (FAB) and electron-impact (EI) mass spectra on VG-ZAB or VG-Autospec instruments, EPR spectra on a Bruker ESP-300E spectrometer either at room temperature or at 77 K, IR spectra as KBr pellets on Carl Zeiss specord M80 or Perkin-Elmer FT-1600 spectrometers and electronic spectra on Shimadzu UV-310 or Perkin-Elmer Lambda 2 spectrometers. Electrochemical experiments were performed using a computer-controlled EG&G-PAR model 273A potentiostat. A conventional three-

† *Supplementary data available:* see Instructions for Authors, *J. Chem. Soc., Dalton Trans.*, 1995, Issue 1, pp. xxv–xxx.

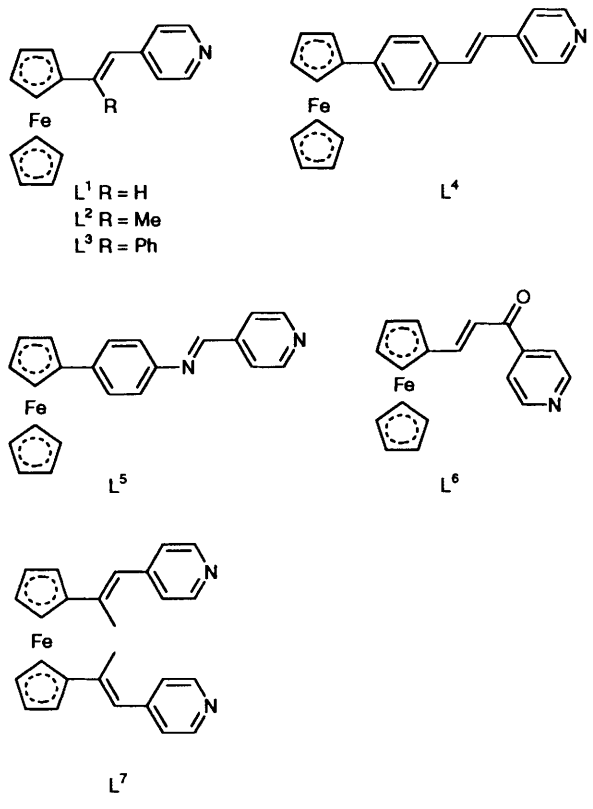

electrode configuration with platinum-bead working and auxiliary electrodes and a saturated calomel reference electrode (SCE) was used. Ferrocene was added at the end of each experiment as an internal standard; all potentials are quote *vs.* the ferrocene–ferrocenium couple. All reaction solvents were dried by standard methods before use.

Starting materials were obtained from Aldrich. 4-Methylpyridine and diisopropylamine were distilled from CaH_2 immediately before use; all other reagents were used as received. Lithium diisopropylamide was prepared *in situ* before use from equivalent amounts of n-butyllithium and diisopropylamine in dry tetrahydrofuran (thf). The complex $[MoL^*(NO)Cl_2]$[29] and 1-(4-formylphenyl)ferrocene[30] were prepared by the published methods.

Syntheses.—L^1. To an ice-cold solution of $Li[NPr^i_2]$ (7.2 mmol) in thf (40 cm^3) under N_2 was added 4-methylpyridine (1 cm^3, 7.0 mmol) in thf (30 cm^3), and the resulting solution was stirred for 1 h. A solution of ferrocenecarbaldehyde (1.5 g, 7.0 mmol) in thf (30 cm^3) was then added dropwise, and the mixture was stirred overnight at room temperature, before quenching with water (10 cm^3). After concentration *in vacuo* the crude intermediate alcohol was obtained as a brown solid after extraction with several portions of CH_2Cl_2, and was used for dehydration without further purification. It was dissolved in dry pyridine (25 cm^3) and a solution of $POCl_3$ (1.44 g, 9.4 mmol) in dry pyridine (10 cm^3) was added dropwise with stirring at room temperature under argon. After stirring for 3 h and quenching with ice the mixture was evaporated to dryness *in vacuo* to give a dark gum. Water (75 cm^3) was then added and the solution made slightly basic with NaOH. The suspension was extracted with several portions of CH_2Cl_2 which were combined, dried ($MgSO_4$) and evaporated to dryness *in vacuo*. Purification by column chromatography on alumina (Brockmann activity V) with CH_2Cl_2–hexane (1 : 1, v/v) afforded pure L^1 in 59% yield as bright red microcrystals.

The following compounds were prepared by the same general method: L^2, from $Li[NPr^i_2]$ (8.9 mmol), 4-methylpyridine (8.8 mmol) and 1-acetylferrocene (8.8 mmol), yield 35%; L^3, from $Li[NPr^i_2]$ (8.8 mmol), 4-methylpyridine (8.8 mmol) and 1-benzoylferrocene (8.6 mmol) (dehydration with $POCl_3$–pyridine required 48 h), yield 22%; L^4, from $Li[NPr^i_2]$ (3.5 mmol), 4-methylpyridine (3.5 mmol) and 1-(4-formylphenyl)ferrocene (3.1 mmol), reaction time 6 h, dehydration with $POCl_3$–pyridine (1 h), final purification on alumina (Brockmann activity V) with CH_2Cl_2 as eluent, yield 76%; L^7 from $Li[NPr^i_2]$ (15 mmol), 4-methylpyridine (15 mmol) and 1,1′-diacetylferrocene (2.03 g, 7.5 mmol), purification by chromatography on alumina (Brockmann activity I) with CH_2Cl_2–MeCN (8.5 : 1.5, v/v) as eluent, second major fraction collected and dried *in vacuo* to give pure L^7 (0.51 g, 15%).

L^5. To a solution containing 4-aminophenylferrocene (0.55 g, 1.9 mmol) and pyridine-4-carbaldehyde (0.30 g, 2.8 mmol) in anhydrous methanol (45 cm^3) was added 4 Å molecular sieves, (*ca.* 1.5 g) upon which a red precipitate appeared. The mixture was refluxed overnight and then concentrated *in vacuo* to 15 cm^3. The suspension was refrigerated and the red solid filtered off, washed with methanol and then diethyl ether, and dried *in vacuo*. Yield: 99%.

L^6. To a solution of ferrocenecarbaldehyde (2.10 g, 9.8 mmol) in dry ethanol (150 cm^3) was added 4-acetylpyridine (1.00 g, 8.3 mmol). The mixture was stirred for 5 min and then aqueous NaOH (28 cm^3 of 2 mol dm^{-3} solution) was added. The mixture was refluxed for 0.5 h, allowed to cool and extracted with several portions of CH_2Cl_2. The combined extracts were dried ($MgSO_4$) and then evaporated to dryness. The mixture was purified by chromatography on alumina (Brockmann activity V) with CH_2Cl_2–hexane (1 : 1, v/v). The first band to elute was unreacted ferrocenecarbaldehyde; L^6 was the second (purple) band to elute. It was recrystallized from EtOH–$CHCl_3$. Yield: 11%.

Analytical and spectroscopic data for L^1–L^7 are summarized in Table 1.

Molybdenum complexes Mo′L^1–Mo′L^6. These were prepared by the same general method, of which that for Mo′L^1 described is representative. A mixture of L^1 (0.28 g, 0.97 mmol), $[MoL^*(NO)Cl_2]$ (0.53 g, 1.06 mmol), dry triethylamine (1 cm^3) and dry toluene (100 cm^3) was heated to reflux under N_2 for 3.5 h, allowed to cool, and evaporated to dryness *in vacuo*. The crude mixture was purified by chromatography on silica. Initial elution with CH_2Cl_2–hexane (9 : 1) eluted traces of unreacted $[MoL^*(NO)Cl_2]$ and a pale green impurity (a μ-oxo binuclear molybdenum complex). Changing the solvent to CH_2Cl_2 containing 1–2% thf allowed elution of the dark red product. Yield: 65%. Yields (%) for the other binuclear complexes: of L^2 (red), 60; L^3 (red), 39; L^4 (red), 63; L^5 (purple), 11; L^6 (purple), 34.

The trinuclear complex Mo′$_2L^7$ was likewise prepared from L^7 (0.06 g, 0.14 mmol), $[MoL^*(NO)Cl_2]$ (0.15 g, 0.31 mmol), and dry triethylamine (1 cm^3) in refluxing toluene–CH_2Cl_2 (9 : 1) (reaction time 6 h) followed by chromatographic purification as described above. Yield: 29%.

Analytical and spectroscopic data for the complexes are summarized in Table 7.

X-Ray Crystallography.—L^1. Enraf-Nonius CAD-4 diffractometer, graphite-monochromatized Cu-Kα radiation (λ = 1.5418 Å), ω–2θ scan mode. The crystal and data collection parameters are given in Table 2. Three reflections were measured periodically as orientation and intensity control and no significant variations were observed. Lorentz, polarization and empirical absorption corrections were applied.[31] The structure was solved by direct methods using MULTAN,[32] and refined by the full-matrix least-squares method on *F* using a PDP-11/73 computer and the SDP package.[33] Selected bond lengths and angles are given in Table 3, atomic coordinates in Table 4.

L^4. Siemens R3m/V diffractometer, graphite-monochromatized Mo-Kα radiation (λ = 0.710 73 Å), Wyckoff ω-scan mode.

Table 1 Spectroscopic and analytical data for the new ferrocenes (cp = cyclopentadienyl)

Compound	Analysis[a] (%) C	H	N	FAB *m/z*	^{1}H NMR (CD_2Cl_2), δ (*J*/Hz)
L^1	70.7 (70.6)	5.2 (5.2)	4.8 (4.8)	289	8.48 (2 H, d, *J* = 6.2, py $H^{2,6}$), 7.28 (2 H, d, *J* = 6.2, py $H^{3,5}$), 7.14 (1 H, d, *J* = 16, CH), 6.62 (1 H, d, *J* = 16, CH), 4.51 (2 H, t, *J* = 1.9, cp' $H^{2,5}$), 4.35 (2 H, t, *J* = 1.9, cp' $H^{3,4}$), 4.15 (5 H, s, cp)[b]
L^2	71.1 (71.3)	5.6 (5.6)	4.6 (4.6)	303	8.51 (2 H, d, *J* = 6.2, py $H^{2,6}$), 7.21 (2 H, d, *J* = 6.2, py $H^{3,5}$), 6.62 (1 H, br s, CH), 4.52 (2 H, t, *J* = 1.8, cp' $H^{2,5}$), 4.32 (2 H, t, *J* = 1.8, cp' $H^{3,4}$), 4.15 (5 H, s, cp), 2.26 (3 H, d, *J* = 1.1, CH_3)[b]
L^3	75.3 (75.6)	5.7 (5.2)	3.9 (3.8)	365	8.24 (2 H, d, *J* = 5.7, py $H^{2,6}$), 7.47–7.41 (3 H, m, Ph H^{3-5}), 7.30 (2 H, m, Ph $H^{2,6}$), 6.81 (1 H, s, CH), 6.72 (2 H, dd, *J* = 4.5 and 1.3, py $H^{3,5}$), 4.33 (4 H, m, cp'), 4.17 (5 H, s, cp)[b]
L^4	75.5 (75.7)	5.3 (5.2)	3.8 (3.8)	365	8.55 (2 H, br s, py $H^{2,6}$), 7.50 (4 H, s, C_6H_4), 7.39 (2 H, d, *J* = 6.1, py $H^{3,5}$), 7.33 (1 H, d, *J* = 16, CH), 7.05 (1 H, d, *J* = 16, CH), 4.70 (2 H, t, *J* = 1.8, cp' $H^{2,5}$), 4.36 (2 H, t, *J* = 1.8, cp' $H^{3,5}$), 4.04 (5 H, s, cp)[b]
L^5	71.4 (72.1)	4.9 (5.0)	8.1 (7.7)	366	8.72 (2 H, dd, *J* = 4.5 and 1.7, py $H^{2,6}$), 8.55 (1 H, s, CH), 7.77 (2 H, dd, *J* = 4.5 and 1.7, py $H^{3,5}$), 7.54 (2 H, dd, *J* = 6.6 and 2.0, C_6H_4), 7.24 (2 H, dd, *J* = 6.6 and 2.0, C_6H_4), 4.69 (2 H, t, *J* = 1.9, cp' $H^{2,5}$), 4.36 (2 H, t, *J* = 1.9, cp' $H^{3,4}$), 4.06 (5 H, s, cp)[b]
L^6	67.2 (67.1)	4.9 (5.3)	4.1 (4.1)	314	8.78 (2 H, dd, *J* = 4.3 and 1.5, py $H^{2,6}$), 7.77 (1 H, d, *J* = 15.4, CH), 7.70 (2 H, dd, *J* = 4.3 and 1.5, py $H^{3,5}$), 7.04 (1 H, d, *J* = 15.4, CH), 4.64 (2 H, t, *J* = 1.9, cp' $H^{2,5}$), 4.55 (2 H, t, *J* = 1.9, cp' $H^{3,4}$), 4.20 (5 H, s, cp)[b]
L^7	74.3 (74.3)	5.7 (5.8)	6.5 (6.7)	420	8.48 (4 H, s, py $H^{2,6}$), 7.13 (4 H, s, py $H^{3,5}$), 6.61 (2 H, s, CH), 4.51 (4 H, s, cp' $H^{2,5}$), 4.34 (4 H, s, cp' $H^{3,4}$), 2.21 (6 H, s, CH_3)[c]

[a] Expected values in parentheses. [b] Spectrum recorded at 270 MHz. [c] Spectrum recorded at 100 MHz.

Table 2 Summary of crystal data, intensity collection and refinement for L^1 and L^4

	L^1	L^4
Formula	$C_{17}H_{15}FeN$	$C_{23}H_{19}FeN$
M	289	365
T/K	293(2)	293(2)
Crystal size/mm	0.28 × 0.40 × 0.03	0.33 × 0.29 × 0.8
Symmetry, space group	Orthorhombic, *Pcab*	Monoclinic, $P2_1$
a/Å	7.724(5)	10.779(4)
b/Å	10.503(2)	7.555(3)
c/Å	33.361(6)	21.234(8)
β/°	90	91.85(3)
U/Å^3	2706.5(18)	1728.3(11)
Z	8	4
D_c/Mg m^{-3}	1.422	1.404
F(000)	1200	760
μ/mm^{-1}	8.8 (Cu-Kα)	0.876 (Mo-Kα)
$2\theta_{max}$ for data collection/°	130	55
Independent reflections	1938	4008
Refinement method	Full-matrix least squares on *F* [1053 data with $I \geqslant 3\sigma(I)$]	Full-matrix least squares on all F^2 data
Final residuals	$R = 0.069$, $R' = 0.088$	$R = 0.061$, $wR2 = 0.140$
Largest difference peak, hole/e Å^{-3}	+0.51, −0.82	+0.36, −0.45

The crystal and data collection parameters are given in Table 2. Three reflections were measured periodically as orientation and intensity control and no significant variations were observed. Lorentz, polarization and empirical absorption corrections were applied.[34] All initial calculations were performed with a DEC micro-Vax II computer with the SHELXTL PLUS system of programs, and the final least-squares refinement on F^2 on a Silicon Graphics Indigo R4000 computer using SHELXL 93.[34] Scattering factors with corrections for anomalous dispersion were taken from ref. 35. Selected bond lengths and angles are given in Table 5, atomic coordinates in Table 6.

Additional material available from the Cambridge Crystallographic Data Centre comprises H-atom coordinates, thermal parameters and remaining bond lengths and angles.

Results and Discussion

The new ferrocene-based compounds L^1–L^4 and L^7 were prepared by condensation of the anion of 4-methylpyridine with the appropriate carbonyl-containing ferrocene derivative; the intermediate alcohols were dehydrated with $POCl_3$–pyridine. The lower electrophilicity of ketones compared to aldehydes partly accounts for the lower yields of L^2, L^3 and L^7 compared to those of L^1 and L^4; in addition we found that the dehydration of the intermediate alcohols was slower and less efficient for L^2, L^3 and L^7 which may be due to the steric effect of the additional substituents at the dehydration site. The Schiff base L^5 was simply prepared by a condensation reaction involving primary amine and carbonyl groups. The analogous reaction between 4-aminopyridine and 1-(4-formylphenyl)ferrocene, which would have yielded the positional isomer of L^5 with the N atom at the other end of the double bond, was unsuccessful, no doubt due to the low basicity of the amino group of 4-aminopyridine. Compound L^6 was prepared in low yield by a conventional aldol-type condensation. The structures of all of the ferrocenes were confirmed by elemental analysis, FAB mass spectrometric and ^{1}H NMR data. In particular the ^{1}H NMR spectra of L^1 and L^4 indicate that only the less-hindered *E* isomers have formed (J = 16 Hz for the *trans* pair of protons on the double bond), and we assume that the other compounds are also formed as the *E* isomers.[36,37]

The crystal structures of L^1 and L^4 have been determined and are shown in Figs. 1 and 2 respectively (Tables 2–6). Both show the same type of disorder in the position of the double bond,

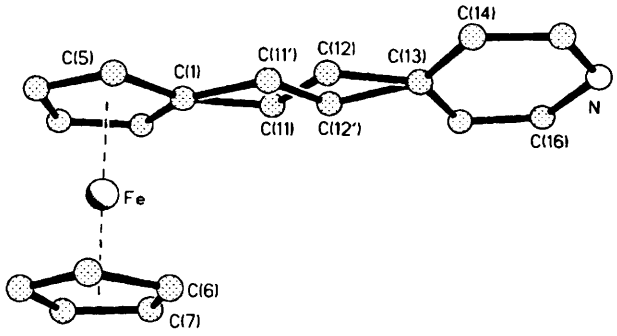

Fig. 1 Crystal structure of L^1 depicting the disorder in the double bond

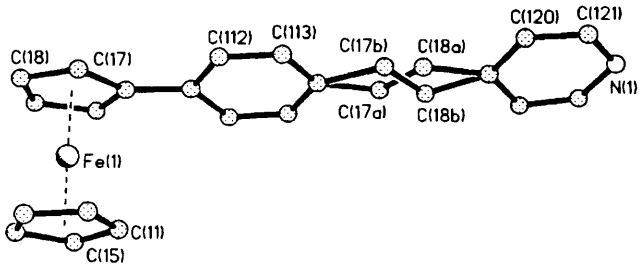

Fig. 2 Crystal structure of L^4 depicting the disorder in the double bond

Table 3 Selected bond lengths (Å) and angles (°) for L^1

Fe–C(1)	2.08(1)	Fe–C(6)	2.03(2)
Fe–C(2)	2.02(2)	Fe–C(7)	2.03(1)
Fe–C(3)	2.03(2)	Fe–C(8)	2.04(2)
Fe–C(4)	2.01(2)	Fe–C(9)	2.02(1)
Fe–C(5)	2.04(1)	Fe–C(10)	2.03(1)
C(1)–C(11)	1.43(1)	C(12)–C(13)	1.48(2)
C(11)–C(12)	1.35(2)		
C(2)–C(1)–C(11)	115.1(9)	C(12)–C(13)–C(14)	110.1(9)
C(11)–C(12)–C(13)	119(2)	C(14)–C(13)–C(17)	116.2(8)
C(1)–C(11)–C(12)	121(2)	C(11)–C(12)–C(13)	119(2)

which results in high positional errors and thermal parameters for the atoms concerned. For L^1 the two positions of the double bond are in a 2 : 1 ratio in the crystal; for L^4 the ratio is 1 : 1. For L^1, although the final R factor is respectable (0.069), both the thermal parameters and the estimated standard deviations in the molecular geometry parameters are large, due principally to the thinness of the crystal and the correspondingly weak data set. In addition the bond lengths and angles involving the disordered atoms are not very precise. A detailed discussion of the structural parameters is therefore inappropriate, but it is clear that the side-arm is nearly coplanar with the cyclopentadienyl ring to which it is attached and that the double bond has the *E* conformation. Compound L^4 crystallizes with two independent molecules in the asymmetric unit. One of these (that depicted) has a similar disorder in the position of the double bond to that observed in L^1, with the two components being present in a 1 : 1 ratio this time; the independent molecule

Table 4 Fractional atomic coordinates (× 10^4) for L^1, with estimated standard deviations (e.s.d.s) in parentheses

Atom	*x*	*y*	*z*
Fe	1834(2)	65(1)	764(1)
N	2010(10)	−1214(7)	3134(2)
C(1)	580(10)	−1037(8)	1191(3)
C(2)	−590(10)	−253(8)	976(3)
C(3)	−550(10)	−480(9)	577(3)
C(4)	660(20)	−1455(9)	516(3)
C(5)	1390(10)	−1811(9)	882(3)
C(6)	3890(10)	932(9)	1028(3)
C(7)	2650(10)	1828(9)	924(3)
C(8)	2430(10)	1784(9)	515(3)
C(9)	3520(10)	827(9)	367(3)
C(10)	4420(10)	297(8)	688(3)
C(11)	650(20)	−800(10)	1614(4)[a]
C(11')	1450(40)	−1480(20)	1585(8)[b]
C(12)	1580(20)	−1560(10)	1859(4)[a]
C(12')	870(40)	−810(20)	1885(7)[b]
C(13)	1620(10)	−1279(9)	2293(3)
C(14)	2520(10)	−2205(8)	2492(3)
C(15)	2680(10)	−2137(8)	2896(3)
C(16)	1150(20)	−312(8)	2928(3)
C(17)	950(10)	−307(8)	2526(3)

[a] Atom refined with site occupancy $\frac{2}{3}$. [b] Atom refined with site occupancy $\frac{1}{3}$.

Table 5 Selected bond lengths (Å) and angles (°) for L^4

Fe(1)–C(11)	2.028(11)	Fe(2)–C(21)	2.056(10)
Fe(1)–C(12)	2.01(2)	Fe(2)–C(22)	2.050(11)
Fe(1)–C(13)	2.03(2)	Fe(2)–C(23)	2.019(11)
Fe(1)–C(14)	2.022(14)	Fe(2)–C(24)	2.034(9)
Fe(1)–C(15)	2.026(11)	Fe(2)–C(25)	2.059(9)
Fe(1)–C(16)	2.036(10)	Fe(2)–C(26)	2.037(10)
Fe(1)–C(17)	2.037(8)	Fe(2)–C(27)	2.031(9)
Fe(1)–C(18)	2.041(11)	Fe(2)–C(28)	2.033(10)
Fe(1)–C(19)	2.020(12)	Fe(2)–C(29)	2.026(12)
Fe(1)–C(110)	2.023(13)	Fe(2)–C(210)	2.028(12)
C(16)–C(111)	1.468(12)	C(26)–C(211)	1.487(12)
C(114)–C(17a)	1.45(2)	C(214)–C(217)	1.480(13)
C(114)–C(17b)	1.59(3)		
C(17a)–C(18a)	1.34(2)	C(217)–C(218)	1.298(13)
C(17b)–C(18b)	1.32(3)		
C(18a)–C(119)	1.52(2)	C(218)–C(219)	1.491(13)
C(18b)–C(119)	1.52(3)		
C(16)–C(111)–C(112)	121.8(8)	C(26)–C(211)–C(212)	122.2(8)
C(16)–C(111)–C(116)	122.4(8)	C(26)–C(211)–C(216)	120.8(8)
C(114)–C(17a)–C(18a)	120(3)	C(214)–C(217)–C(218)	126.5(10)
C(114)–C(17b)–C(18b)	115(2)		
C(119)–C(18a)–C(17a)	121(2)	C(219)–C(218)–C(217)	126.0(10)
C(119)–C(18b)–C(17b)	112(2)		

Table 6 Fractional atomic coordinates ($\times 10^4$) for L^4, with e.s.d.s in parentheses

Atom	x	y	z	Atom	x	y	z
Fe(1)	1228(1)	0	1192(1)	C(124)	−51(12)	−2145(16)	5907(6)
C(11)	−197(14)	1300(24)	1587(6)	Fe(2)	6298(1)	4741(2)	1177(1)
C(12)	702(17)	2423(23)	1467(10)	C(21)	7006(9)	6712(16)	1751(5)
C(13)	902(15)	2476(26)	858(12)	C(22)	6507(10)	7437(15)	1194(7)
C(14)	150(18)	1338(31)	557(7)	C(23)	7124(10)	6675(17)	686(5)
C(15)	−586(11)	561(21)	1010(11)	C(24)	8022(8)	5506(15)	925(5)
C(16)	2063(8)	−1551(14)	1866(4)	C(25)	7965(9)	5496(16)	1595(5)
C(17)	2963(7)	−540(17)	1550(4)	C(26)	5045(8)	3281(16)	1652(4)
C(18)	2886(10)	−957(20)	902(5)	C(27)	4457(8)	4162(18)	1134(5)
C(19)	1955(10)	−2203(18)	810(5)	C(28)	5036(10)	3594(22)	572(5)
C(110)	1411(9)	−2609(17)	1388(6)	C(29)	5964(11)	2381(18)	751(6)
C(111)	1830(7)	−1523(11)	2543(4)	C(210)	5976(10)	2182(16)	1409(6)
C(112)	2643(8)	−710(13)	2972(4)	C(211)	4720(7)	3432(11)	2325(4)
C(113)	2458(11)	−713(15)	3609(5)	C(212)	5369(8)	2532(13)	2800(5)
C(114)	1447(14)	−1574(16)	3859(5)	C(213)	5040(9)	2586(16)	3423(5)
C(115)	624(12)	−2381(18)	3436(6)	C(214)	4003(8)	3651(13)	3598(4)
C(116)	790(8)	−2346(14)	2799(5)	C(215)	3363(8)	4542(15)	3126(4)
C(17A)	958(22)	−1865(27)	4477(9)*	C(216)	3712(7)	4465(13)	2503(4)
C(18A)	1517(20)	−1142(25)	4986(8)*	C(217)	3604(9)	3820(14)	4256(5)
C(17B)	1650(20)	−1235(29)	4592(12)*	C(218)	4158(9)	3154(14)	4754(5)
C(18B)	728(17)	−1737(30)	4946(11)*	C(219)	3766(9)	3373(12)	5416(4)
C(119)	1019(13)	−1430(16)	5641(5)	C(220)	4496(9)	2672(14)	5893(5)
C(120)	1876(10)	−764(16)	6057(5)	C(221)	4149(9)	2813(15)	6497(5)
C(121)	1699(10)	−821(15)	6689(5)	N(2)	3114(8)	3619(12)	6679(4)
N(1)	725(8)	−1529(13)	6955(4)	C(223)	2392(8)	4323(14)	6219(5)
C(123)	−135(11)	−2186(19)	6547(7)	C(224)	2683(9)	4245(13)	5587(4)

* Atom refined with 50% site occupancy.

Table 7 Analytical and spectroscopic data for the new complexes

	Analysis* (%)				FAB*	
Complex	C	H	N	$\tilde{\nu}_{NO}/cm^{-1}$	m/z	g_{iso} (A_{Mo}/mT)
Mo'L^1	51.8 (51.4)	4.8 (5.0)	14.8 (15.0)	1605	749 (749)	1.978 (4.8)
Mo'L^2	52.4 (52.0)	5.5 (5.2)	15.1 (14.7)	1606	763 (763)	1.978 (4.8)
Mo'L^3	55.2 (55.4)	5.0 (5.0)	13.6 (13.6)	1605	825 (825)	1.978 (4.7)
Mo'L^4	55.5 (55.4)	5.4 (5.0)	13.8 (13.6)	1600	825 (825)	1.978 (4.8)
Mo'L^5	53.9 (53.9)	5.4 (4.9)	15.1 (15.3)	1615	826 (826)	1.978 (4.7)
Mo'L^6	51.1 (51.1)	5.3 (4.8)	14.5 (14.4)	1606	777 (777)	1.978 (4.7)
$Mo_2'L^7$	50.7 (50.3)	5.1 (5.1)	16.6 (16.8)	1605	1335 (1335)	See text

* Expected values in parentheses.

Table 8 Electrochemical data

	$E_{\frac{1}{2}}$/V (ΔE_p/mV)[a]		
Compound	Mo(18e–17e)	Mo(17e–16e)	Ferrocenyl
Mo'L^1	−1.94 (90)	+0.01[b]	+0.10[b]
Mo'L^2	−1.97 (75)	+0.02[b]	+0.10[b]
Mo'L^3	−1.92 (95)	+0.02 (100)	+0.15 (100)
Mo'L^4	−1.86 (90)	+0.04 (90)[c]	
Mo'L^5	−1.63 (100)	−0.04 (200)[c]	
Mo'L^6	−1.47 (100)	+0.02[b]	+0.08[b]
$Mo_2'L^7$	−1.94 (150)[d]	+0.02 (75)[d]	+0.19 (75)

Values for ferrocenyl moiety of free ferrocene derivatives; L^1, $E_{\frac{1}{2}}$ +0.05 (ΔE_p 80); L^2, +0.05 (100); L^3, +0.07 (85); L^4, +0.03 (65); L^5, +0.08 (80); L^6, +0.04, +0.16 (see footnote *b*); L^7; +0.18 V (100 mV). [a] All measurements made in CH_2Cl_2 containing 0.2 mol dm^{-3} $NBu^n_4PF_6$ at a platinum-bead working electrode. All potentials are *vs.* the ferrocene–ferrocenium couple. [b] Peak resolved in square-wave voltammogram so ΔE_p value not available. [c] Coincident oxidations of molybdenum and ferrocenyl fragments not resolved. [d] Two simultaneous one-electron processes, for both molybdenum centres.

however has no disorder and is well defined, with a near-planar side-arm and an *E* double bond. In both L^1 and L^4 therefore there is considerable π-electron overlap between the side chain and the cyclopentadienyl ring to which it is attached. The extent of this π interaction between ferrocenyl cores and attached substituents is known to vary significantly with the nature of the side chains.[18]

The 16 valence-electron molybdenum complex [MoL*-$(NO)Cl_2$] reacts with pyridine or substituted pyridines to form the corresponding 17-electron pyridyl derivatives.[26–28,37] We have used this reaction to synthesize the binuclear complexes Mo'L^1–Mo'L^6 and the trinuclear complex Mo'_2L^7 [where Mo' denotes the {MoL*(NO)Cl} fragment attached to the pyridyl arms of L^1–L^7]. The formulations of the complexes were confirmed by elemental analysis and FAB mass spectroscopy. In addition the attachment of a pyridyl ligand to the {MoL*(NO)Cl} core is confirmed by the shift in the position of ν_{NO} in the IR spectra, from 1718 cm^{-1} for [MoL*-$(NO)Cl_2$] to around 1605 cm^{-1} for the pyridyl-substituted products.[26–28,37]

Electrochemistry.—The electrochemical results are summarized in Table 8. The substituted ferrocenes L^1–L^7 undergo reversible one-electron oxidations at potentials slightly more anodic than that of unsubstituted ferrocene; similar anodic shifts have also been reported for two different terpyridyl derivatives[21,24] and can be attributed to the conjugation of the ferrocenyl unit to the electron-deficient pyridyl group. By 'reversible' is meant that the anodic and cathodic peak currents

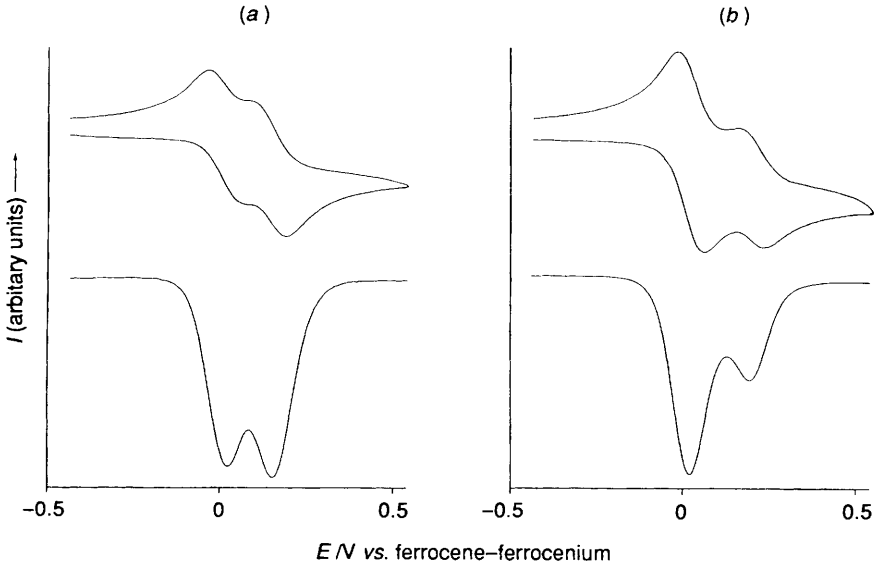

Fig. 3 Cyclic and square-wave voltammograms of (*a*) Mo'L^6 and (*b*) Mo'$_2$L^7

Table 9 The UV/VIS spectral data for L^1–L^7 recorded in CH_2Cl_2

Compound	λ_{max}/nm (10^{-3} ε/dm^3 mol^{-1} cm^{-1})			
L^1	466 (1.9)	373 (3.3)	313 (26)	266 (15)
L^2	453 (1.0)	362 (2.3)	306 (15)	265 (12)
L^3	474 (2.2)	378 (3.6)	317 (25)	266 (16)
L^4	453 (1.7)	383 (4.6)	333 (21)	Not resolved
L^5	467 (2.0)	348 (1.0)	285 (16)	243 (21)
L^6	523 (2.8)	396 (2.0)	329 (12)	Not resolved
L^7	505 (1.7)	370 (4.0)	305 (13)	265 (10)

are equal and the peak-to-peak separation ΔE_p lies in the range 60–100 mV. For ferrocene under the same conditions ΔE_p was typically 80 mV. Compound L^6 undergoes an oxidation of the carboxypyridine moiety in addition to the ferrocenyl redox process; although the peak potentials could be extracted from a square-wave voltammogram, their reversibility and ΔE_p values could not be obtained from a cyclic voltammogram since the two processes overlap closely.

In the binuclear complexes Mo'L^1–Mo'L^6 the molybdenum (17e–16e) and ferrocenyl-based couples are close together resulting in two overlapping waves in the cyclic voltammograms. Square-wave voltammetry successfully resolved the two processes for Mo'L^1–Mo'L^3 and Mo'L^6 [Fig. 3(*a*)], but for Mo'L^4 and Mo'L^5 the processes are superimposed and cannot be individually resolved. It is not immediately apparent for Mo'L^1–Mo'L^3 and Mo'L^6 which oxidation belongs to the ferrocenyl moiety and which to the molybdenum moiety, but examination of the electrochemical properties of the trinuclear complex Mo'$_2$L^7 makes it clear [Fig. 3(*b*)]. For this complex the first oxidation, at +0.02 V, is approximately twice as intense as the second at +0.19 V. This is only consistent with the first wave being two coincident 17e–16e couples, and is to be expected since we have observed before that the Mo-based 17e–16e couples in binuclear complexes do not split but are always coincident.[26–28] All seven complexes also show the expected Mo-based 17e–18e couples. For Mo'$_2$L^7 this corresponds to two near-coincident one-electron transfers, and the slight broadening of the wave (ΔE_p = 150 mV in the cyclic voltammogram) indicates a degree of interaction between the two processes even though the combined wave cannot be resolved into two components.

Since the molybdenum fragment oxidizes before the ferrocenyl fragment, the ferrocenyl redox potential will be affected by the presence of a positively charged molybdenum fragment attached to the pendant pyridyl substituent. For Mo'L^1–Mo'L^3 the anodic shifts of the ferrocenyl redox couples (compared to the precursors L^1–L^3) are 50, 50 and 80 mV respectively. For Mo'$_2$L^7 the effect is approximately doubled compared to Mo'L^2, with an anodic shift of 90 mV. The ferrocenyl fragment is therefore sensitive to the presence of fairly remote substituents attached *via* conjugated linking groups; the magnitudes of the shifts are comparable to those of other complexes where ferrocenyl groups have been used as redox spectators.[7–11,19–25] In contrast the molybdenum-based 16e–17e couples are essentially invariant throughout the series of complexes. However the molybdenum-based 17e–18e couples are sensitive to the nature of remote ligand substituents, since the reductions are substantially delocalized onto the bridging ligand. In accordance with this Mo'L^5 and Mo'L^6, which have highly electronegative atoms in the conjugated networks, are the easiest to reduce. Likewise Mo'L^4 is easier to reduce than Mo'L^1–Mo'L^3 as the pyridyl substituent is more highly conjugated and the π^* orbitals are therefore lower in energy.

Electronic Spectroscopy.—Unsubstituted ferrocene exhibits two bands at 325 and 440 nm in the electronic spectrum, which have been assigned to $^1A_{2g} \longrightarrow {}^1E_{2g}$ and $^1A_{1g} \longrightarrow {}^1E_{1g}$ ligand-field (d–d) transitions. An intense transition at 200 nm arises from ligand-to-metal charge transfer, and two shoulders at 240 and 265 nm are also thought to arise from some form of charge-transfer process.[38] Upon substitution of a cyclopentadienyl ring with conjugated acceptor groups, it is expected that (*i*) cyclopentadienyl orbitals will shift to lower energy, and (*ii*) there will be increased mixing of ligand orbitals with the metal d orbitals.

Both of these effects are apparent in the spectra of L^1–L^7 (Table 9). The two lowest-energy transitions are substantially red-shifted with respect to unsubstituted ferrocene, and the intensities of the transitions are also very much greater (ε > 1000 dm^3 mol^{-1} cm^{-1} for these transitions of L^1–L^7 compared to < 50 for ferrocene) since increased mixing of metal and ligand orbitals means that the d–d transitions now have a significant ligand character and become more 'allowed'. By analogy with related ferrocene derivatives bearing electron-accepting substituents linked *via* polyene chains,[16] the lowest unoccupied molecular orbital (LUMO) is no longer a metal d orbital but is a π^* orbital delocalized over the conjugated side-group: accordingly the lowest-energy transition is no longer

d–d, but is a metal-to-ligand charge transfer (m.l.c.t.) band with some d–d character. The second lowest transition is now a ligand-centred π–π^* transition involving the conjugated side-group, also mixed with some d–d character. The increase in the extent of conjugation in L^7 as compared to L^2 is responsible for further decrease in the energy of the LUMO (π^*) orbital, which is reflected in the additional red shift of the lowest-energy m.l.c.t. absorption band. The ketonic substituent of L^6 results in a particularly low energy for the first m.l.c.t. band, which has been noticed for related ferrocene derivatives.[39,40] The two more-intense transitions at higher energy are also red-shifted compared to ferrocene[38] and are therefore also likely to have m.l.c.t. character.

The {MoL*(NO)(pyridyl)Cl} chromophore has a characteristic molybdenum-to-pyridyl m.l.c.t. band in the visible region, the position of which is sensitive to the presence of substituents on the pyridyl ligand.[26–28,37] In the spectra of the complexes $Mo'L^1$–$Mo'L^6$ and Mo'_2L^7 in CH_2Cl_2 (Table 10) however this Mo-based transition is generally masked by the ferrocenyl m.l.c.t. band, although for $Mo'L^4$, $Mo'L^5$ and Mo'_2L^7 it is just visible as a shoulder on the low-energy side of the ferrocenyl m.l.c.t. band. Attachment of the 17-valence electron {MoL*(NO)Cl} fragment to the pendant pyridyl binding sites of L^1–L^7 has resulted in a red shift of *ca.* 50 nm in every case: the {MoL*(NO)Cl} substituent therefore acts as an electron-accepting group and lowers the energy of the π^* orbital with which it is conjugated. The electrochemical results described above showed that the oxidized $\{MoL^*(NO)Cl\}^+$ substituents acted as electron-accepting groups, which is not surprising, but these electronic spectral results show that the neutral {MoL*(NO)Cl} substituent also has electron-accepting character.

Since both the Mo- and the ferrocenyl-based m.l.c.t. transitions have charge-transfer character they may be solvatochromic, and the electronic spectra of a selection of the complexes were therefore recorded in a variety of solvents of different relative permittivities. The results are in Table 11. In polar solvents such as MeCN the two bands are not resolved but appear as a single broad absorption. As the relative permittivity of the medium is decreased the ferrocenyl-based m.l.c.t. band varies in position in a rather unpredictable manner, but the Mo-based m.l.c.t. band is steadily red-shifted, and develops a weak low-energy shoulder (Fig. 4) which becomes more pronounced the weaker is the relative permittivity of the solvent. In very low-polarity solvents a third low-energy transition may become discernible (Fig. 4). Although a multiparameter model of solvent polarity, taking into account solvent dipolarity, hydrogen-bond donating and accepting ability and solvent polarizability, is sometimes used to interpret solvatochromic data,[41,42] the negative solvatochromism of the molybdenum-to-pyridine m.l.c.t. band is quite clear using solvent relative permittivity alone as a measure of polarity, as is established practice.[43,44] The negative solvatochromism means that in this case the ground state is more polar than the excited state. Owing to the large solvent effect it is not possible to estimate the effect of the ferrocenyl substituent on the Mo-based m.l.c.t. band. The lowest-energy π–π^* transition of L^1–L^7, at around 350–400 nm (Table 9), is not resolved for $Mo'L^1$–$Mo'L^6$ and Mo'_2L^7 as it is obscured by the more intense band at 320–370 nm. We ascribe this latter transition to a charge-transfer process of some sort involving the bridging ligand group because of (*i*) its high intensity, (*ii*) the variation in its energy with the nature of the conjugated linker, and (*iii*) its weak positive solvatochromism (*e.g.* for $Mo'L^1$ it varies from 315 nm in hexane to 332 nm in dimethylformamide).

EPR Properties.—The binuclear complexes $Mo'L^1$–$Mo'L^6$, which contain one 17-electron molybdenum centre, show characteristic[26–28,37] isotropic solution spectra with $g_{av} = 1.978(1)$ and a hyperfine splitting $A_{Mo} = 4.8(1)$ mT [Fig. 5(*a*)]. Earlier studies have shown that for binuclear 17-electron molybdenum complexes with bridging ligands such as 4,4′-bipyridine there is a magnetic exchange interaction between the two unpaired electrons.[26–28] Provided that $|J| \gg A_{Mo}$, where $2J$ is the singlet–triplet separation, this results in a 'fast-exchange' spectrum in which both electrons are apparently coupled to both nuclei: the separation between hyperfine components halves to 2.4 mT and a pattern characteristic of coupling to two equivalent nuclei with $I = \frac{5}{2}$ appears.

In Mo'_2L^7 the pathway linking the two paramagnetic groups is longer than we have used before and the resulting EPR spectrum [Fig. 5(*b*)] is characteristic of $|J| \approx A_{Mo}$.[45] In this intermediate domain the appearance of the second-order spectrum is very sensitive to the value of $|J|$, the magnitude of which may therefore be determined by spectral simulation. Although we could not duplicate the appearance of this spectrum exactly its appearance is best accounted for with $|J| \approx 2000$ MHz (taking A_{Mo} to be 140 MHz). In contrast a 'fast-exchange' spectrum occurs for $|J| > 5000$ MHz, and the 'slow-exchange' limit to give a spectrum like those of mononuclear complexes requires $|J| < 10$ MHz. For Mo'_2L^7 the interaction is therefore just below the limit required for 'fast exchange'. By analogy with other binuclear complexes bridged by 4,4′-bipyridyl-type bridges,[27,46] J is negative and the interaction is weakly antiferromagnetic. This is generally consistent with the electrochemical results which indicate that although there is a significant interaction between the ferrocenyl and pendant molybdenum groups, the two molybdenum groups interact (at best) very weakly.

Table 10 The UV/VIS spectroscopic data for the new complexes in CH_2Cl_2

Complex	λ_{max}/nm (10^{-3} ε/dm^3 mol^{-1} cm^{-1})			
$Mo'L^1$	277 (14)	329 (21)	512 (5.7)	
$Mo'L^2$	278 (6.9)	323 (8.2)	489 (2.0)	
$Mo'L^3$	278 (15)	334 (18)	516 (4.8)	
$Mo'L^4$	279 (6.2)	356 (11)	496 (3.1)	570 (sh)
$Mo'L^5$	284 (9.5)	372 (6.0)	530 (2.3)	570 (sh)
$Mo'L^6$	281 (7.9)	334 (6.2)	568 (2.0)	
Mo'_2L^7	276 (11)	334 (12)	486 (4.0)	530 (sh)

Table 11 Solvatochromism of the m.l.c.t. bands of some of the complexes (dmf = dimethylformamide, thf = tetrahydrofuran)

	λ_{max}/nm								
Complex	MeCN	dmf	MeOH	Acetone	CH_2Cl_2	thf	Et_2O	Benzene	Hexane
$Mo'L^1$	508	512	513	506	512	501	502	498	493 (sh)
						550 (sh)	555 (sh)	550 (sh)	577
$Mo'L^4$	486	493	490	491	496	497	501	506	510
				560 (sh)	570 (sh)	570 (sh)	570	580	580
$Mo'L^5$	512	521	500	520	530	524	510	521	494 (sh)
				565 (sh)	570 (sh)	570 (sh)	590	588	621
$Mo'L^6$	556	564	526	556	568	556	553	560	539
							585 (sh)	590 (sh)	610 (sh)

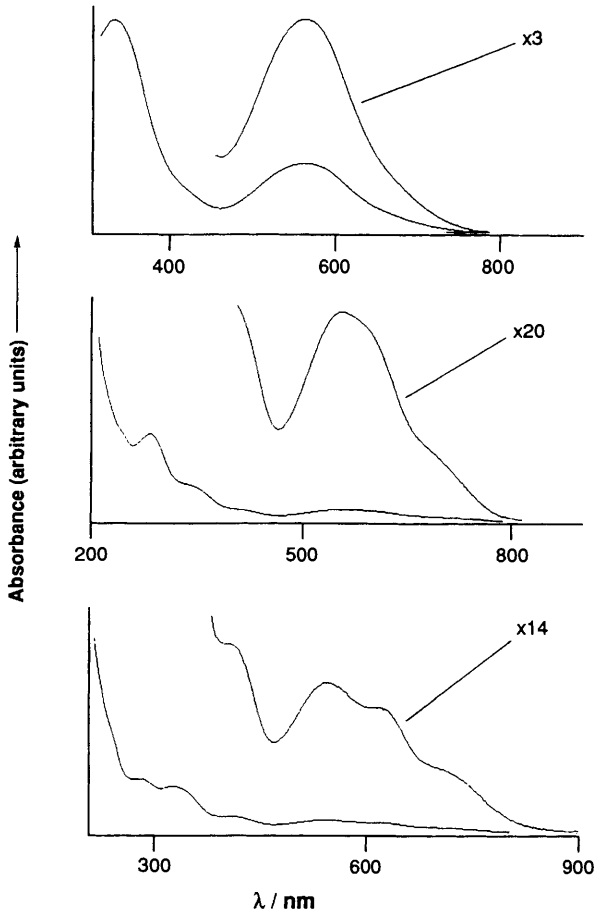

Fig. 4 The UV/VIS spectra of Mo'L[6] in (from top downwards) acetone, diethyl ether, and hexane, showing the splitting of the m.l.c.t. band into separate components as the solvent polarity decreases

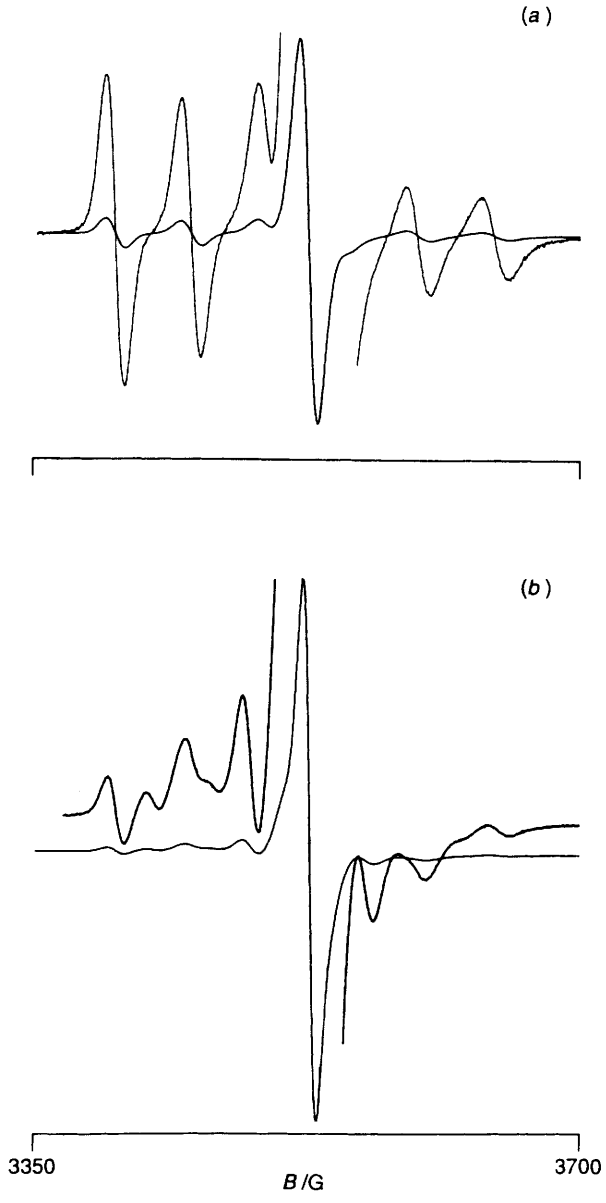

Fig. 5 Solution EPR spectra of (*a*) Mo'L[4] and (*b*) Mo'$_2$L[7]. Expansions are × 10

Conclusion

We have prepared a series of new ferrocene derivatives with pendant pyridyl groups to which {MoL*(NO)Cl} fragments were attached. Electrochemical and UV/VIS spectroscopic measurements indicate that the {MoL*(NO)Cl} fragment acts as an electron-accepting group, making the ferrocenyl redox couple more anodic and lowering the energy of the bridging-ligand based π* orbital. In Mo'$_2$L[7] there is an electronic interaction between the ferrocenyl core and the two pendant {MoL*(NO)Cl} fragments, but the two {MoL*(NO)Cl} are too remote from each other to have a significant electrochemical effect on each other. However there is a very weak magnetic exchange interaction between them characterized by $|J| \approx 2000$ MHz as determined from the EPR spectrum.

These complexes also fulfil the basic requirements for materials with non-linear optical (NLO) properties: they contain ferrocene as a donor group, {MoL*(NO)Cl} as an acceptor group, and a conjugated polarizable bridge linking the two fragments. Complexes similar to these have been shown to display significant NLO effects.[14] We are currently attempting to measure the NLO properties of these new complexes and the results will be reported in due course.

Acknowledgements

We thank the EPSRC for a research studentship (to J. A. N. B.) and funds to purchase the EPR spectrometer, and Dr. John Maher for assistance with the EPR spectra. A. D. and M. M. B. gratefully thank Professor P. Natarajan, Director of the Central Salt and Marine Chemicals Research Institute, for his keen interest in the part of the work done there.

References

1 *Inorganic Materials*, eds. D. W. Bruce and D. O'Hare, Wiley, Chichester, 1992.
2 I. Hawkins, R. A. Clark, C. E. Waunwrite and A. E. Underhill, *Mol. Cryst. Liq. Cryst.*, 1990, **181**, 209.
3 I. R. Butler, *Specialist Periodical Report – Organometallic Chemistry*, ed. E. W. Abel, Cambridge, 1992, vol. 21, ch. 14.
4 C. Kollmar, M. Conty and D. Kahn, *J. Am. Chem. Soc.*, 1991, **113**, 7994.
5 K. M. Chi, J. C. Calabrese, W. M. Reiff and J. S. Miller, *Organometallics*, 1991, **10**, 668.
6 K. S. Narayan, B. G. Morin, J. S. Miller and A. J. Epstein, *Phys. Rev. B*, 1992, **46**, 6195.
7 E. C. Constable, *Angew. Chem., Int. Ed. Engl.*, 1991, **30**, 407.
8 R. W. Wagner, P. A. Brown, T. E. Johnson and J. S. Lindsey, *J. Chem. Soc., Chem. Commun.*, 1991, 1463.
9 M. C. B. Colbert, S. L. Ingham, J. Lewis, N. J. Long and P. R. Raithby, *J. Chem. Soc., Dalton Trans.*, 1994, 2215.
10 P. D. Beer, C. Blackburn, J. F. McAleer and H. Sikanyika, *Inorg. Chem.*, 1990, **29**, 378.
11 P. D. Beer, *Chem. Soc. Rev.*, 1989, **18**, 409.
12 M. W. Laidlaw, R. G. Denning, T. Verbiest, E. Chanchard and A. Persoons, *Nature (London)*, 1993, **363**, 58.

13 B. J. Coe, C. J. Jones, J. A. McCleverty, D. Bloor, P. V. Kolinsky and R. J. Jones, *J. Chem. Soc., Chem. Commun.*, 1989, 1485.
14 B. J. Coe, J.-D. Foulon, T. A. Hamor, C. J. Jones, J. A. McCleverty, D. Bloor, G. H. Cross and T. L. Axon, *J. Chem. Soc., Dalton Trans.*, 1994, 3427.
15 D. R. Kanis, M. A. Ratner and T. J. Marks, *J. Am. Chem. Soc.*, 1992, **114**, 10338; *Chem. Rev.*, 1994, **94**, 195.
16 J. C. Calabrese, L.-T. Cheng, J. C. Green, S. R. Marder and W. Tam, *J. Am. Chem. Soc.*, 1991, **113**, 7227.
17 S. R. Marder, J. W. Perry, B. G. Tiemann and W. P. Schaefer, *Organometallics*, 1991, **10**, 1896.
18 A. Togni and G. Rihs, *Organometallics*, 1993, **12**, 3368.
19 R. Bosque, M. F. Bardia, C. Lopez, J. Sales, J. Silver and X. Solans, *J. Chem. Soc., Dalton Trans.*, 1994, 747.
20 R. Bosque, L. Lopez, J. Sales, X. Solans and M. F. Bardia, *J. Chem. Soc., Dalton Trans.*, 1994, 735.
21 E. C. Constable, A. J. Edwards, R. M. Manez, P. R. Raithby and A. M. W. Cargill Thompson, *J. Chem. Soc., Dalton Trans.*, 1994, 645.
22 E. C. Constable, R. M. Manez, A. M. W. Cargill Thompson and J. V. Walker, *J. Chem. Soc., Dalton Trans.*, 1994, 1585.
23 P. D. Beer, O. Kocian, R. J. Mortimer and P. Spencer, *J. Chem. Soc., Dalton Trans.*, 1990, 3283.
24 J.-C. Chambron, C. Coudret and J.-P Sauvage, *New J. Chem.*, 1992, **16**, 1361.
25 T. M. Miller, K. J. Ahmed and M. S. Wrighton, *Inorg. Chem.*, 1989, **28**, 2347.
26 S. L. W. McWhinnie, C. J. Jones, J. A. McCleverty, F. E. Mabbs and D. Collison, *J. Chem. Soc., Chem. Commun.*, 1990, 940.
27 J. A. Thomas, C. J. Jones, J. A. McCleverty, D. Collison, F. E. Mabbs, C. J. Harding and M. G. Hutchings, *J. Chem. Soc., Chem. Commun.*, 1992, 1796.
28 A. Das, J. P. Maher, J. A. McCleverty, J. A. Navas Badiola and M. D. Ward, *J. Chem. Soc., Dalton Trans.*, 1993, 681.
29 C. J. Jones, J. A. McCleverty, S. J. Reynolds and C. F. Smith, *Inorg. Synth.*, 1985, **23**, 4.
30 B. J. Coe, Ph.D, Thesis, University of Birmingham, 1991.
31 A. C. T. North, D. C. Phillips and E. S. Mathews, *Acta Crystallogr., Sect. A*, 1968, **24**, 351.
32 P. Mann, MULTAN 11/82, University of York, 1982.
33 B. A. Frenz and associates, SDP Structure Determination Package, College Station, TX; Enraf-Nonius, Delft, 1985.
34 SHELXTL PLUS program system (S320), Nicolet Instrument Corporation, Madison, WI, 1987; SHELXL 93 program system, Siemens Analytical X-Ray Instruments, Madison, WI, 1993.
35 *International Tables for X-Ray Crystallography*, Kynoch Press, Birmingham, 1974, vol. 4.
36 R. J. Shaw, R. T. Webb and R. H. Schmehl, *J. Am. Chem. Soc.*, 1990, **112**, 1117.
37 A. Das, J. C. Jeffery, J. P. Maher, J. A. McCleverty, E. Schatz, M. D. Ward and G. Wollermann, *Inorg. Chem.*, 1993, **32**, 2145.
38 Y. S. Sohn, D. N. Hendrickson and H. B. Gray, *J. Am. Chem. Soc.*, 1971, **93**, 3603.
39 S. Toma, A. Gáplovský and I. Pavlík, *Monatsh. Chem.*, 1985, **116**, 479.
40 S. Toma, A. Gáplovský, M. Hudecek and Z. Langfelderová, *Monatsh. Chem.*, 1985, **116**, 357.
41 M. J. Kamlet, J.-L. M. Abboud and R. W. Taft, *Prog. Phys. Org. Chem.*, 1981, **13**, 485.
42 R. W. Taft and M. J. Kamlet, *Inorg. Chem.*, 1983, **22**, 250.
43 C. Reichardt, *Solvents and Solvent Effects in Organic Chemistry*, VCH, Weinheim, 1990.
44 W. Kaim, S. Kohlmann, S. Earnst, B. Olbrich-Deussner, C. Bassenbachert and A. Schultz, *J. Organomet. Chem.*, 1987, **321**, 215.
45 R. Cook, J. P. Maher, J. A. McCleverty, M. D. Ward and A. Wlodarczyk, *Polyhedron*, 1993, **12**, 2111.
46 D. Gatteschi, J. A. McCleverty, J. A. Navas Badiola and M. D. Ward, unpublished work.

Received 29*th March* 1995; *Paper* 5/01981H